

Driven-dissipative Rydberg blockade in optical lattices

Javad Kazemi^{1,*} and Hendrik Weimer^{1,†}

¹*Institut für Theoretische Physik, Leibniz Universität Hannover, Appelstraße 2, 30167 Hannover, Germany*

While dissipative Rydberg gases exhibit unique possibilities to tune dissipation and interaction properties, very little is known about the quantum many-body physics of such long-range interacting open quantum systems. We theoretically analyze the steady state of a van der Waals interacting Rydberg gas in an optical lattice based on a variational treatment that also includes long-range correlations necessary to describe the physics of the Rydberg blockade, i.e., the inhibition of neighboring Rydberg excitations by strong interactions. In contrast to the ground state phase diagram, we find that the steady state undergoes a single first order phase transition from a blocked Rydberg gas to a facilitation phase where the blockade is lifted. The first order line terminates in a critical point when including sufficiently strong dephasing, enabling a highly promising route to study dissipative criticality in these systems. In some regimes, we also find good quantitative agreement with effective short-range models despite the presence of the Rydberg blockade, justifying the wide use of such phenomenological descriptions in the literature.

Strongly interacting Rydberg atoms undergoing driving and dissipation allow to study a wide range of many-body effects not seen in their equilibrium counterparts, ranging from dissipative quantum sensors [1] to self-organizing dynamics [2]. These effects are enabled by the presence of a strong van der Waals interaction between the atoms, which is fundamentally long-ranged. Yet, very little is known about the many-body properties of such systems, as long-ranged open quantum systems are inherently hard to simulate on classical computers [3]. Here, we present a variational calculation of the steady state phase diagram of a long-range interacting Rydberg in an optical lattice.

A key feature of strongly interacting Rydberg gases is the appearance of the Rydberg blockade, where the strong van der Waals interactions prevents the excitation of neighboring Rydberg atoms [4–9]. However, given the intrinsic challenges associated with the treatment of open quantum many-body systems, most works studying dissipative Rydberg gases have employed short-range interactions [10–16], which are inadequate for strongly blocked Rydberg gases. As a consequence, the steady state phase diagram of blocked Rydberg gases is essentially unknown.

In this Letter, we present the application of a variational approach for the non-equilibrium steady state of Rydberg atoms with strong repulsive van der Waals interactions. Notably, we explicitly account for correlations between multiple Rydberg excitations. Based upon the variational results, we find a dissipative variant of the Rydberg blockade in the pair correlation function, where any simultaneous excitation within a certain blockade radius is strongly suppressed. In addition, we investigate the interplay between coherent driving and dissipation, finding a first-order dissipative phase transition, which terminates in a critical point under sufficiently strong additional dephasing. Finally, we analyze the validity of effective short-range models to describe the dynamics even in the blocked regime, where we find that such

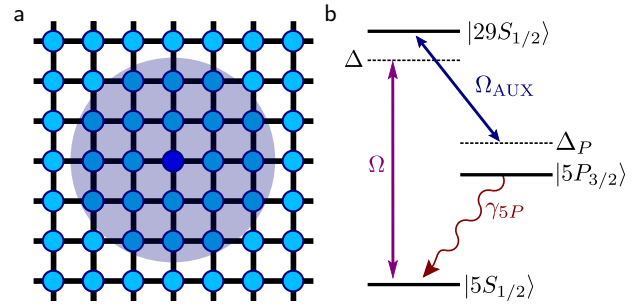


FIG. 1. Setup of the system. (a) Strong van der Waals repulsion leads to a blockade of simultaneous Rydberg excitations over a number of sites of the square lattice. (b) Internal level structure showing a two-photon excitation of a single Rydberg state with a Rabi frequency Ω and a detuning Δ , as well as laser-assisted dissipation via an intermediate excited state.

effective models actually perform better in the presence of a strong Rydberg blockade.

Model. — Dissipative processes involving electronic excitations can often be described in terms of a Markovian master equation in Lindblad form as the frequency of the emitted photons provides for a natural separation of timescales required for the Markov approximation [17]. Then, the time evolution of the density matrix ρ is given by

$$\mathcal{L}(\rho) = -i[H, \rho] + \sum_j \left[c_j \rho c_j^\dagger - \frac{1}{2} \{ c_j^\dagger c_j, \rho \} \right], \quad (1)$$

where \mathcal{L} denotes the Liouvillian superoperator $\mathcal{L}(\rho) = \partial_t \rho$, which consists of a coherent part represented by the Hamiltonian H and a dissipative part characterised a set of jump operators c_j . The coherent dynamics of a ground state atom being laser driven to a single Rydberg state can be expressed in a spin 1/2 Hamiltonian as

$$H = -\frac{\hbar\Delta}{2} \sum_i \sigma_z^{(i)} + \frac{\hbar\Omega}{2} \sum_i \sigma_x^{(i)} + C_6 \sum_{i<j} \frac{P_r^{(i)} P_r^{(j)}}{r_{ij}^6}, \quad (2)$$

where Ω is the driving strength, Δ is the detuning from the atomic resonance, and C_6 denotes the strength of the repulsive van der Waals interaction [18, 19] involving the projector $P_r^{(i)}$ onto the Rydberg state. In our work, we consider the atoms being loaded in a two-dimensional optical lattice, see Fig. 1. The derivation of the jump operators c_j is more subtle [20], but laser-assisted dissipation via an intermediate electronic excitation allows to use effective jump operators of the form $c_j = \sqrt{\gamma}\sigma_-^{(j)}$, with γ being the effective decay rate from the Rydberg state into the ground state [21]. Furthermore, this setup has the advantage that it allows to tune the dissipation rate independently from the other properties of the Rydberg state such as the C_6 coefficient. Here, we also assume that the laser-mediated decay is much faster than the natural decay of the Rydberg excitation or changes in the Rydberg state by blackbody radiation, therefore we neglect these processes. In addition to the dissipation, we also allow for a second set of jump operators $c'_j = \sqrt{\gamma_p}\sigma_z^{(j)}$, where γ_p denotes a dephasing rate arising, e.g., from noise of the driving laser.

Concerning the experimental setup, we consider a square optical lattice trapping Rubidium-87 atoms with a lattice spacing of $a = 532$ nm. Here, we consider laser driving from the electronic ground state by a two-photon transition to the state $|29S_{1/2}\rangle$, which has a van der Waals coefficient of $C_6 = h \times 17 \text{ MHz } \mu\text{m}^6$ [22].

Variational treatment of long-range correlations.— In the following, we will be interested in the properties of the non-equilibrium steady state given by the condition $\partial_t \rho = 0$. Following the variational principle for steady states of open quantum systems [11], we turn to a variational parametrization that also allows for long-range correlations, which are crucial to capture the physics of the Rydberg blockade. For the trial state, we consider a variational ansatz containing local density matrices as well as two-body correlations in the following form

$$\rho_{\text{var}} = \prod_{i=1}^N \rho_i + \sum_{i < j} \mathcal{R} C_{ij}, \quad (3)$$

where N is the number of sites, \mathcal{R} is a superoperator transforming the identity matrix \mathbb{I}_i into ρ_i , and $C_{ij} = \rho_{ij} - \rho_i \otimes \rho_j$ denotes the two-particle correlations. Crucially, we ignore higher-order correlations as in dissipative dynamics with power-law interactions they decay faster than two-body correlations [23]. Considering the residual dynamics of the ansatz, we define a variational cost function that can be cast into the form

$$F_v \equiv N^{-1} \frac{\|\dot{\rho}_{\text{var}}\|_{\text{HS}}^2}{\|\rho_{\text{var}}\|_{\text{HS}}^2}, \quad (4)$$

where $\|O\|_{\text{HS}} = \sqrt{\text{Tr}[OO^\dagger]}$ is the Hilbert-Schmidt norm. Using the definition of F_v for a transnationally invariant system, and expanding the Liouvillian in terms of local

and interacting terms, i.e. $\mathcal{L} = \sum_i \mathcal{L}_i + \sum_{i < j} \mathcal{L}_{ij}$, we end up with an efficiently computable upper bound, i.e. $F_v \leq f_v$, that reads as

$$\begin{aligned} f_v = & g_p^{-2} \sum_{1 \neq j} \langle \rho_{\text{var}}^{(1j)} | \mathcal{L}_1^\dagger \mathcal{L}_1 + \mathcal{L}_1^\dagger \mathcal{L}_j | \rho_{\text{var}}^{(1j)} \rangle \\ & + g_p^{-3} \sum_{1 \neq j \neq k} \langle \rho_{\text{var}}^{(1jk)} | 2\mathcal{L}_1^\dagger \mathcal{L}_{1j} + \mathcal{L}_1^\dagger \mathcal{L}_{jk} | \rho_{\text{var}}^{(1jk)} \rangle \\ & + g_p^{-4} \sum_{1 \neq j \neq k \neq l} \langle \rho_{\text{var}}^{(1jkl)} | \frac{1}{2} \mathcal{L}_{1j}^\dagger \mathcal{L}_{1j} + \frac{1}{2} \mathcal{L}_{1j}^\dagger \mathcal{L}_{jk} \\ & \quad + \frac{1}{2} \mathcal{L}_{1j}^\dagger \mathcal{L}_{lk} + \frac{1}{4} \mathcal{L}_{1j}^\dagger \mathcal{L}_{kl} | \rho_{\text{var}}^{(1jkl)} \rangle, \end{aligned} \quad (5)$$

where we used the notation $\|\dot{\rho}_{\text{var}}\|_{\text{HS}}^2 = \langle \mathcal{L}^\dagger(\rho_{\text{var}}) | \mathcal{L}(\rho_{\text{var}}) \rangle$, and $g_p = \langle \rho_1 | \rho_1 \rangle$ denotes the local purity [21].

Within this approach, we can also make statements about systems in the thermodynamic limit, even for finite N . This is possible, as within our variational approach, a system of N sites is indistinguishable from an infinitely large system in which correlations over a cluster of N sites are accounted for. Hence, we can easily detect the presence of dissipative phase transitions by observing non-analytic behavior of steady state observables. Note that while our approach shares some similarities to previous approaches based on cluster mean-field theory [24, 25], the variational character allows us to avoid some pitfalls associated with mean-field theory in open systems [11, 26, 27].

A crucial aspect of our variational approach is to accurately describe the pair correlation function $g_2(r_{ij}) = \langle P_r^{(i)} P_r^{(j)} \rangle / \langle P_r^{(i)} \rangle \langle P_r^{(j)} \rangle$ with relatively few variational parameters that need to be optimized. From perturbation theory in the strongly blockaded regime [28], one can expect that the pair correlation function behaves for small distances as $g_2(r_{ij}) \sim r_{ij}^6$, while for weak interactions at large interactions, one would expect $\lim_{r_{ij} \rightarrow \infty} g_2(r_{ij}) = 1$. An expansion satisfying these two limits is given by

$$g_2(r) = \frac{\alpha_6 r^6}{\alpha_6 r^6 + \sum_{0 \leq k < 6} \alpha_k r^k}, \quad (6)$$

where the α_k are variational parameters. Here, we truncate the sum after the second order, for which we find that Eq. (6) is in good quantitative agreement with exact numerical simulations of small systems. For correlation functions involving σ_x or σ_y , we assume an exponential decay, with the only exception being the correlator $\langle \sigma_y^{(i)} \sigma_z^{(j)} \rangle - \langle \sigma_y^{(i)} \rangle \langle \sigma_z^{(j)} \rangle$, which is inherently linked to $g_2(r)$ through the Lindblad master equation [21].

Steady state phase diagram.— First, we focus on the case without any dephasing, i.e., $\gamma_p = 0$. Without any dissipation, the ground state phase diagram of Eq. (2) on a lattice for $\Delta > 0$ consists of a series of crystalline

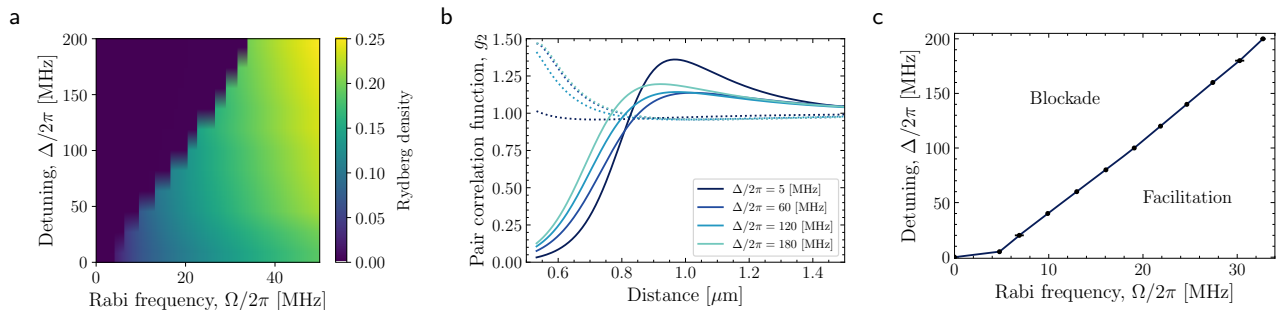


FIG. 2. Variational results for the steady state of two-dimensional driven Rydberg gases in the presence of decay with the rate $\gamma = 2\pi \times 1$ MHz. (a). Rydberg density obtained from a cluster size of 9×9 exhibits a discontinuity for different values of detuning Δ signalling a first-order transition, with the step-like discreteness being due to the numerical resolution. (b) The pair correlation function g_2 demonstrates a blocked region for low-density phase (solid lines) and a facilitated region for high-density phase (dotted lines). In all cases, the driving strength Ω was chosen right below the transition (solid) or right above it (dotted) (c) The steady-state phase diagram is obtained by finite-size scaling of the variational results which resembles a lattice liquid-gas transition.

phases that can be either commensurate or incommensurate with the underlying lattice, and a paramagnetic phase for sufficiently strong driving strength Ω [29–31]. Including dissipation, we find a vastly different phase diagram for the nonequilibrium steady state. Overall, we find the presence of two competing phases, see Fig. 2, one at low densities exhibiting the characteristic pair correlation function $g_2(r)$ of the Rydberg blockade, and one at higher densities in which the Rydberg atoms are either uncorrelated or even exhibiting bunching of neighboring Rydberg excitations, i.e., leading to a complete lifting of the Rydberg blockade. We note that the second phase continuously connects to the so-called anti-blockade or facilitated regime [32–34], where the detuning cancels the longitudinal field term arising from the interaction, resulting in an effectively purely transversal Ising model. Hence, we refer to the two phases as “blockade phase” and “facilitation phase”, respectively. We find that the two phases are separated by a first order transition that stretches throughout the entire parameter space. To determine the position of the first-order line in the limit of infinitely large clusters, we perform an analysis in close analogy to finite-size scaling, using cluster sizes of 5×5 , 7×7 , and 9×9 . The choice of odd numbers is twofold; First, it considerably simplifies the expressions for the variational norm as it can be constructed around a site at the center of the lattice. Second, even and odd sites have slightly different scaling behavior, so focusing on only one of them achieves faster convergence. The result of the cluster scaling analysis is shown in Fig. 2c. Furthermore, even in the facilitation phase, we find that the density of Rydberg excitations is comparatively low close to the transition, which we attribute to the first excitation still being suppressed by the van der Waals interaction, which is much stronger than the driving strength Ω . Remarkably, in stark contrast to the ground state

phase diagram, we find no evidence for consumerability effects with the underlying lattice, as the first order line appears to be a smooth function, with other quantities such as the blockade radius behaving in a similar way.

Dephasing-induced criticality.— Without dephasing, the numerical results are consistent with the first order line extending all the way to $\Delta = 0$, without triggering any critical behavior, in contrast to both the ground state phase diagram and the steady-state phase diagram for purely coherent evolution [35, 36]. However, as already known from other dissipative models exhibiting first-order transitions [12, 37, 38], such first order lines between two competing phases can be turned critical by injecting additional dephasing noise into the dynamics. Within our variational approach, we also observe this behavior for the long-range interacting case, see Fig. 3a. In particular, we find the critical point emerging for a detuning of $\Delta = 2\pi \times 40$ MHz at $\gamma_p = 2\pi \times 16$ MHz. Such a level dephasing can be realized experimentally by noise on the excitation laser, opening a very promising route to study dissipative criticality in such a setting.

Effective short range models.— As already mentioned, the inherent challenges with studying open quantum many-body systems has led to most theoretical works replacing the long-range interaction in dissipative Rydberg gases by a short-range interaction. While it is clear that this is inadequate to correctly describe the Rydberg blockade, one may ask whether such a simplification can still be used to describe dissipative Rydberg gases, especially since properly renormalized short-range models have had some success in describing experiments even in the blocked regime [12]. To this end, we develop a systematic way to derive effective short-range models [21]. Here, we consider the situation where the detuning is chosen in such a way that it realizes an anti-blockade configuration at a particular distance r' . Then, we assume

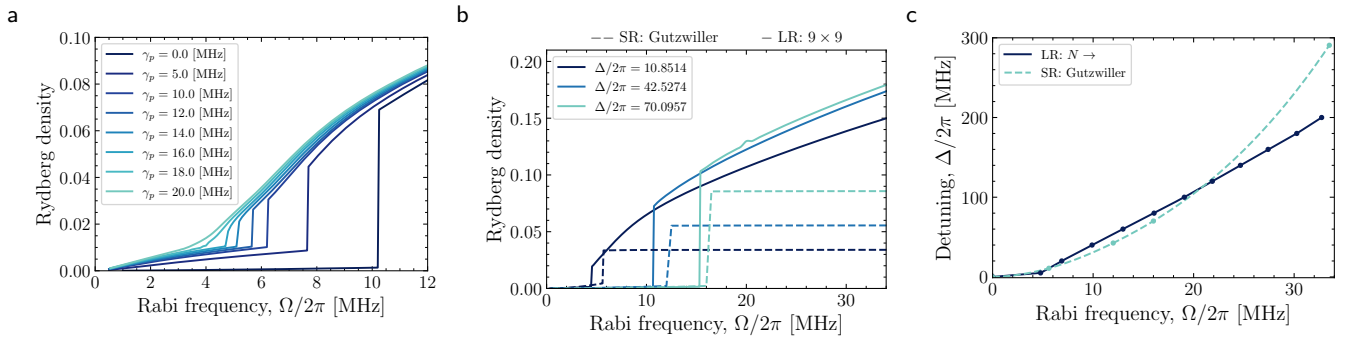


FIG. 3. Extensions to the basic model. (a) Inclusion of dephasing results in the termination of the first order line with a critical point. For $\Delta = 2\pi \times 40$ MHz, criticality appears at $\gamma_p = 2\pi \times 16$ MHz. (b) Variational results for an effective short-range interacting model using a Gutzwiller ansatz (dashed lines) in comparison with the long-range interacting model using the correlated ansatz (solid lines). (c) For relatively weak driving, the phase transition in dissipative Rydberg gases can be effectively described by a short-range interacting model.

that all lattice sites in between are effectively frozen and consider an effective model involving only the remaining sites. As we operate in an anti-blockade configuration, we obtain a purely transversal Ising model, i.e.,

$$H_{\text{eff}} = \frac{\hbar\Omega}{2} \sum_i \sigma_x^{(i)} + J_{\text{eff}}(r_d) \sum_{\langle ij \rangle} \sigma_z^{(i)} \sigma_z^{(j)}, \quad (7)$$

where $J_{\text{eff}}(r_d)$ denotes the strength of the nearest-neighbor Ising interaction which accounts for van der Waals interaction excluding terms from the nearest-neighbor up to a truncation distance $r_d < r'$ [21].

We can benchmark the validity of the effective short-range model by performing variational calculations. For the short-range model, we utilize a Gutzwiller ansatz, which has been shown to give reliable quantitative estimates of the position of the first order transition [16]. Fig. 3b-c confirms that the short-range Ising model is in good quantitative agreement with the long-range interacting model after accounting for the number of excluded sites by rescaling the Rydberg density by a factor of $(r_d + 1)^2$, provided that the driving strength Ω is relatively small. For larger values of the driving strength, resulting in a decreasing truncation radius r_d , the correspondence becomes worse, although the position of the first order transition remains quite accurate over a substantially larger region. This is somewhat counterintuitive, as in the limit where the truncation distance vanishes, one would expect a short-range model to be valid, although there are cases when considering classical rate equations instead of a Lindblad master equation, where a van der Waals interactions is not decaying sufficiently fast to allow for a replacement by a nearest-neighbor interaction [39].

In summary, we have analyzed the stationary properties of strongly interacting Rydberg gases under driving and dissipation using a variational treatment properly capturing long-range correlations. In stark contrast to

the ground state phase diagram, the steady state of dissipative Rydberg gases features a single first-order phase transition between a blockaded phase and a facilitation phase, without any commensurability effects from the underlying optical lattice. The first-order line can be tuned critical by incorporating additional dephasing noise, leading to a very promising route to investigate dissipative criticality in an open quantum system. Finally, we find that despite strong blockade effects, effective short-range descriptions of dissipative Rydberg gases can be successfully used to explain the basic features of the steady state phase diagram and hence can serve as a minimal model.

We thank C. Groß, P. Schauf, and J. Zeiher for valuable discussions on the experimental realization of dissipative Rydberg gases. This work was funded by the Volkswagen Foundation, by the Deutsche Forschungsgemeinschaft (DFG, German Research Foundation) within SFB 1227 (DQ-mat, project A04), SPP 1929 (GiRyd), and under Germanys Excellence Strategy – EXC-2123 QuantumFrontiers – 90837967.

* javad.kazemi@itp.uni-hannover.de

† hweimer@itp.uni-hannover.de

- [1] C. G. Wade, M. Marcuzzi, E. Levi, J. M. Kondo, I. Lesanovsky, C. S. Adams, and K. J. Weatherill, Terahertz-driven phase transition applied as a room-temperature terahertz detector, [arXiv:1709.00262 \(2017\)](#).
- [2] S. Helmrich, A. Arias, G. Lochead, T. M. Wintermantel, M. Buchhold, S. Diehl, and S. Whitlock, Signatures of self-organized criticality in an ultracold atomic gas, *Nature* **577**, 481 (2020).
- [3] H. Weimer, A. Kshetrimayum, and R. Orús, Simulation methods for open quantum many-body systems, *Rev. Mod. Phys.* **93**, 015008 (2021).
- [4] D. Jaksch, J. I. Cirac, P. Zoller, S. L. Rolston, R. Côté,

- and M. D. Lukin, Fast Quantum Gates for Neutral Atoms, *Phys. Rev. Lett.* **85**, 2208 (2000).
- [5] M. D. Lukin, M. Fleischhauer, R. Côté, L. M. Duan, D. Jaksch, J. I. Cirac, and P. Zoller, Dipole Blockade and Quantum Information Processing in Mesoscopic Atomic Ensembles, *Phys. Rev. Lett.* **87**, 037901 (2001).
- [6] K. Singer, M. Reetz-Lamour, T. Amthor, L. G. Marcassa, and M. Weidemüller, Suppression of Excitation and Spectral Broadening Induced by Interactions in a Cold Gas of Rydberg Atoms, *Phys. Rev. Lett.* **93**, 163001 (2004).
- [7] R. Heidemann, U. Raitzsch, V. Bendkowsky, B. Butscher, R. Löw, L. Santos, and T. Pfau, Evidence for Coherent Collective Rydberg Excitation in the Strong Blockade Regime, *Phys. Rev. Lett.* **99**, 163601 (2007).
- [8] P. Schauß, M. Cheneau, M. Endres, T. Fukuhara, S. Hild, A. Omran, T. Pohl, C. Gross, S. Kuhr, and I. Bloch, Observation of spatially ordered structures in a two-dimensional Rydberg gas, *Nature* **491**, 87 (2012).
- [9] H. Bernien, S. Schwartz, A. Keesling, H. Levine, A. Omran, H. Pichler, S. Choi, A. S. Zibrov, M. Endres, M. Greiner, *et al.*, Probing many-body dynamics on a 51-atom quantum simulator, *Nature* **551**, 579 (2017).
- [10] T. E. Lee and M. C. Cross, Spatiotemporal dynamics of quantum jumps with Rydberg atoms, *Phys. Rev. A* **85**, 063822 (2012).
- [11] H. Weimer, Variational Principle for Steady States of Dissipative Quantum Many-Body Systems, *Phys. Rev. Lett.* **114**, 040402 (2015).
- [12] H. Weimer, Variational analysis of driven-dissipative Rydberg gases, *Phys. Rev. A* **91**, 063401 (2015).
- [13] A. Kshetrimayum, H. Weimer, and R. Orús, A simple tensor network algorithm for two-dimensional steady states, *Nature Commun.* **8**, 1291 (2017).
- [14] J. Panas, M. Pasek, A. Dhar, T. Qin, A. Geißler, M. Hafez-Torbati, M. E. Sorantin, I. Titvinidze, and W. Hofstetter, Density-wave steady-state phase of dissipative ultracold fermions with nearest-neighbor interactions, *Phys. Rev. B* **99**, 115125 (2019).
- [15] V. P. Singh and H. Weimer, Driven-Dissipative Criticality within the Discrete Truncated Wigner Approximation, *Phys. Rev. Lett.* **128**, 200602 (2022).
- [16] J. Kazemi and H. Weimer, Genuine Bistability in Open Quantum Many-Body Systems, [arXiv:2111.05352](https://arxiv.org/abs/2111.05352) (2021).
- [17] H.-P. Breuer and F. Petruccione, *The Theory of Open Quantum Systems* (Oxford University Press, Oxford, 2002).
- [18] F. Robicheaux and J. V. Hernández, Many-body wave function in a dipole blockade configuration, *Phys. Rev. A* **72**, 063403 (2005).
- [19] R. Löw, H. Weimer, J. Nipper, J. B. Balewski, B. Butscher, H. P. Büchler, and T. Pfau, An experimental and theoretical guide to strongly interacting Rydberg gases, *Journal of Physics B: Atomic, Molecular and Optical Physics* **45**, 113001 (2012).
- [20] C. Nill, K. Brandner, B. Olmos, F. Carollo, and I. Lesanovsky, Many-body radiative decay in strongly interacting Rydberg ensembles (2022), [arXiv:2206.02843](https://arxiv.org/abs/2206.02843) [quant-ph].
- [21] See the Supplemental Material for a derivation of the effectively local jump operators, the details of the variational ansatz, and the derivation of the effective short-range model.
- [22] S. Weber, C. Tresp, H. Menke, A. Urvoy, O. Firstenberg, H. P. Büchler, and S. Hofferberth, Tutorial: Calculation of Rydberg interaction potentials, *J. Phys. B* **50**, 133001 (2017).
- [23] P. Navez and R. Schützhold, Emergence of coherence in the Mott-insulator–superfluid quench of the Bose-Hubbard model, *Phys. Rev. A* **82**, 063603 (2010).
- [24] J. Jin, A. Biella, O. Viyuela, L. Mazza, J. Keeling, R. Fazio, and D. Rossini, Cluster Mean-Field Approach to the Steady-State Phase Diagram of Dissipative Spin Systems, *Phys. Rev. X* **6**, 031011 (2016).
- [25] J. Jin, A. Biella, O. Viyuela, C. Ciuti, R. Fazio, and D. Rossini, Phase diagram of the dissipative quantum Ising model on a square lattice, *Phys. Rev. B* **98**, 241108(R) (2018).
- [26] M. F. Maghrebi and A. V. Gorshkov, Nonequilibrium many-body steady states via Keldysh formalism, *Phys. Rev. B* **93**, 014307 (2016).
- [27] V. R. Overbeck, M. F. Maghrebi, A. V. Gorshkov, and H. Weimer, Multicritical behavior in dissipative Ising models, *Phys. Rev. A* **95**, 042133 (2017).
- [28] M. Müller, I. Lesanovsky, H. Weimer, H. P. Büchler, and P. Zoller, Mesoscopic Rydberg Gate Based on Electromagnetically Induced Transparency, *Phys. Rev. Lett.* **102**, 170502 (2009).
- [29] H. Weimer and H. P. Büchler, Two-Stage Melting in Systems of Strongly Interacting Rydberg Atoms, *Phys. Rev. Lett.* **105**, 230403 (2010).
- [30] B. Capogrosso-Sansone, C. Trefzger, M. Lewenstein, P. Zoller, and G. Pupillo, Quantum Phases of Cold Polar Molecules in 2D Optical Lattices, *Phys. Rev. Lett.* **104**, 125301 (2010).
- [31] E. Sela, M. Punk, and M. Garst, Dislocation-mediated melting of one-dimensional Rydberg crystals, *Phys. Rev. B* **84**, 085434 (2011).
- [32] C. Ates, T. Pohl, T. Pattard, and J. M. Rost, Many-body theory of excitation dynamics in an ultracold Rydberg gas, *Phys. Rev. A* **76**, 013413 (2007).
- [33] A. Urvoy, F. Ripka, I. Lesanovsky, D. Booth, J. P. Shaffer, T. Pfau, and R. Löw, Strongly Correlated Growth of Rydberg Aggregates in a Vapor Cell, *Phys. Rev. Lett.* **114**, 203002 (2015).
- [34] M. M. Valado, C. Simonelli, M. D. Hoogerland, I. Lesanovsky, J. P. Garrahan, E. Arimondo, D. Ciampini, and O. Morsch, Experimental observation of controllable kinetic constraints in a cold atomic gas, *Phys. Rev. A* **93**, 040701(R) (2016).
- [35] H. Weimer, R. Löw, T. Pfau, and H. P. Büchler, Quantum Critical Behavior in Strongly Interacting Rydberg Gases, *Phys. Rev. Lett.* **101**, 250601 (2008).
- [36] R. Löw, H. Weimer, U. Krohn, R. Heidemann, V. Bendkowsky, B. Butscher, H. P. Büchler, and T. Pfau, Universal scaling in a strongly interacting Rydberg gas, *Phys. Rev. A* **80**, 033422 (2009).
- [37] M. Marcuzzi, E. Levi, S. Diehl, J. P. Garrahan, and I. Lesanovsky, Universal Nonequilibrium Properties of Dissipative Rydberg Gases, *Phys. Rev. Lett.* **113**, 210401 (2014).
- [38] M. Raghunandan, J. Wrachtrup, and H. Weimer, High-Density Quantum Sensing with Dissipative First Order Transitions, *Phys. Rev. Lett.* **120**, 150501 (2018).
- [39] M. Hoening, W. Abdussalam, M. Fleischhauer, and T. Pohl, Antiferromagnetic long-range order in dissipative Rydberg lattices, *Phys. Rev. A* **90**, 021603(R) (2014).

Supplemental Material for “Driven-Dissipative Rydberg Blockade in Optical Lattices”

Javad Kazemi^{1,*} and Hendrik Weimer^{1,†}

¹*Institut für Theoretische Physik, Leibniz Universität Hannover, Appelstraße 2, 30167 Hannover, Germany*

S.1. EFFECTIVE LOCAL JUMP OPERATORS FOR INTERACTING RYDBERG ATOMS

In many phenomenological descriptions of dissipative Rydberg gases, the dissipation is incorporated in terms of local jump operators connecting the Rydberg state to the ground state. While this is a reasonable assumption for non-interacting atoms, the presence of strong van der Waals interactions can modify this picture, as the frequency of emitted photons generically contains information about the local surroundings of the emission site [1]. However, when using a setup involving laser-assisted dissipation, see Fig. 1b of the main text, one can justify the use of local jump operators, as we show below.

Without loss of generality, we consider a subsystem of three Rydberg atoms with three electronic levels for each atom, $\{|g_i\rangle, |p_i\rangle, |r_i\rangle\}$. For simplicity, we also neglect the laser driving between the ground state and the Rydberg state, as this occurs on a much slower timescale. Then, the Hamiltonian is of the form

$$H_{\text{Ryd}} = \Omega_{\text{AUX}} \sum_{i=1}^3 (|p_i\rangle\langle r_i| + |r_i\rangle\langle p_i|) + \Delta_p \sum_{i=1}^3 |p_i\rangle\langle p_i| + V_{rr} \sum_{\langle ij \rangle} |r_i r_j\rangle\langle r_i r_j|, \quad (\text{S1})$$

where $\langle ij \rangle \in \{12, 23\}$ due to the assumption of open boundary conditions. We also consider a spontaneously decay from the intermediate state $|p_i\rangle$ to the ground state $|g_i\rangle$, i.e.

$$c_i = \sqrt{\gamma_p} |g_i\rangle\langle p_i|, \quad (\text{S2})$$

where γ_p denotes the decay rate. In the following, we apply the effective operator formalism [2] to eliminate the intermediate states and obtain effective jump operators only involving the ground and Rydberg states. For this, we divide the Hilbert space of our model into a ground-state subspace \mathcal{H}_{gr} , and an excited-state subspace \mathcal{H}_e . Accordingly, one can decompose the Hamiltonian as follows

$$\begin{aligned} H_{\text{Ryd}} &= (P_{gr} + P_e) H_{\text{Ryd}} (P_{gr} + P_e) \\ &= \underbrace{P_{gr} H_{\text{Ryd}} P_{gr}}_{H_{gr}} + \underbrace{P_e H_{\text{Ryd}} P_e}_{H_e} + \underbrace{P_e H_{\text{Ryd}} P_{gr}}_{V_+} + \underbrace{P_{gr} H_{\text{Ryd}} P_e}_{V_-}, \end{aligned} \quad (\text{S3})$$

where $V = V_+ + V_-$ couples the subspaces and the projection operator $P_{gr} = \mathbb{1} - P_e$ is defined as $P_{gr} = \mathbb{1}_{gr}^{(1)} \otimes \mathbb{1}_{gr}^{(2)} \otimes \mathbb{1}_{gr}^{(3)}$ with $\mathbb{1}_{gr}^{(i)} \equiv |g_i\rangle\langle g_i| + |r_i\rangle\langle r_i|$.

The next step is to diagonalize the Hamiltonian H_{gr} in the form of $H_{gr} = \sum_l E_l P_l$, see Table I. Let us express V_+ in terms of the basis P_l such that $V_+ = \sum_l V_+ P_l \equiv \sum_l V_+^l$. Following the procedure in Ref. [2], one can obtain an effective Hamiltonian and effective jump operators given by

$$H_{\text{eff}} = -\frac{1}{2} V_- \sum_l \left[(O_{\text{NH}}^l)^{-1} + ((O_{\text{NH}}^l)^{-1})^\dagger \right] V_+^l + H_{gr}, \quad (\text{S4})$$

$$c_{\text{eff}}^{(m)} = c_m \sum_l (O_{\text{NH}}^l)^{-1} V_+^l, \quad (\text{S5})$$

where $O_{\text{NH}}^{(l)}$ is a non-Hermitian operator which is defined as $O_{\text{NH}}^{(l)} = H_e - i/2 \sum_k c_k c_k^\dagger - E_l$, which in our case reads

$$O_{\text{NH}}^{(l)} = \sum_{m=1}^3 (\Delta_p - E_l - i\frac{\gamma_p}{2}) |p_m\rangle\langle p_m| \otimes \mathbb{1}_{gr} \otimes \mathbb{1}_{gr} + V_{rr} (|prr\rangle\langle prr| + |rrp\rangle\langle rrp|).$$

* javad.kazemi@itp.uni-hannover.de

† hweimer@itp.uni-hannover.de

Eigenstates of H_{gr}	Eigenvalues of H_{gr}	Coupling operator V_+
$P_0 = ggg\rangle\langle ggg $	$E_0 = 0$	$V_+^0 = 0$
$P_1 = rgg\rangle\langle rgg $	$E_1 = 0$	$V_+^1 = \Omega_{\text{AUX}} pgg\rangle\langle rgg $
$P_2 = grg\rangle\langle grg $	$E_2 = 0$	$V_+^2 = \Omega_{\text{AUX}} pgg\rangle\langle grg $
$P_3 = ggr\rangle\langle ggr $	$E_3 = 0$	$V_+^3 = \Omega_{\text{AUX}} gpp\rangle\langle ggr $
$P_4 = rgr\rangle\langle rgr $	$E_4 = 0$	$V_+^4 = \Omega_{\text{AUX}}(pgg\rangle + rpg\rangle)\langle rgr $
$P_5 = rrg\rangle\langle rrg $	$E_5 = V_{rr}$	$V_+^5 = \Omega_{\text{AUX}}(prg\rangle + rpg\rangle)\langle rrg $
$P_6 = grr\rangle\langle grr $	$E_6 = V_{rr}$	$V_+^6 = \Omega_{\text{AUX}}(gpr\rangle + grr\rangle)\langle grr $
$P_7 = rrr\rangle\langle rrr $	$E_7 = 2V_{rr}$	$V_+^7 = \Omega_{\text{AUX}}(prr\rangle + rpr\rangle + rrp\rangle)\langle rrr $

TABLE I. Diagonalization of the ground-state Hamiltonian H_{gr} and the decomposition of the coupling operator V_+ .

The effective process consists of an initial process V_+^l from the state l , an intermediate propagation O_{NH} in the dissipative subspace, and eventually either a coherent process V_- to the reduced subspace corresponding to the effective Hamiltonian, or a decay to $|g_m\rangle$ representing the effective jump operators. In our case, the effective Hamiltonian and jump operators take the form

$$H_{\text{eff}} = V_{rr} \sum_{\langle ij \rangle} |r_i r_j\rangle\langle r_i r_j| - \Omega_{\text{AUX}}^2 \sum_m \frac{\Omega_{i \rightarrow f}}{\Omega_{i \rightarrow f}^2 + \gamma_p^2/4} |r_m\rangle\langle r_m|, \quad (\text{S6})$$

$$c_{\text{eff}}^{(m)} = \frac{\Omega_{\text{AUX}} \sqrt{\gamma_p}}{\Omega_{i \rightarrow f} - i\gamma_p/2} |g_m\rangle\langle r_m|, \quad (\text{S7})$$

where $\Omega_{i \rightarrow f} = \Delta_p + (\tilde{\delta}_{|f\rangle} - \tilde{\delta}_{|i\rangle}) V_{rr}$ is a prefactor depending on the underlying state transition $|f\rangle\langle i|$ such that

$$\tilde{\delta}_{|i\rangle} = \begin{cases} 2 & \text{if } |i\rangle = |rrr\rangle, \\ 1 & \text{if } |i\rangle \in \{|grr\rangle, |rrg\rangle\}, \\ 0 & \text{otherwise.} \end{cases} \quad \text{and} \quad \tilde{\delta}_{|f\rangle} = \begin{cases} 1 & \text{if } |f\rangle \in \{|pr\rangle, |rrp\rangle\}, \\ 0 & \text{otherwise,} \end{cases}$$

To be explicit, the effective jump operators are given by

$$\begin{aligned} c_{\text{eff}}^1 &= \Omega_{\text{AUX}} \sqrt{\gamma_p} [\lambda_1 |ggg\rangle\langle rgg| + \lambda_1 |ggr\rangle\langle rgr| + \lambda_2 |grg\rangle\langle rrg| + \lambda_2 |grr\rangle\langle rrr|], \\ c_{\text{eff}}^2 &= \Omega_{\text{AUX}} \sqrt{\gamma_p} [\lambda_1 |ggg\rangle\langle grg| + \lambda_2 |rgg\rangle\langle rrg| + \lambda_2 |ggr\rangle\langle grr| + \lambda_3 |rgr\rangle\langle rrr|], \\ c_{\text{eff}}^3 &= \Omega_{\text{AUX}} \sqrt{\gamma_p} [\lambda_1 |ggg\rangle\langle ggr| + \lambda_1 |rgg\rangle\langle rgr| + \lambda_2 |grg\rangle\langle grr| + \lambda_2 |rrg\rangle\langle rrr|], \end{aligned}$$

where

$$\begin{aligned} \lambda_1 &= (\Delta_p - i\gamma/2)^{-1}, \\ \lambda_2 &= (\Delta_p - V_{rr} - i\gamma/2)^{-1}, \\ \lambda_3 &= (\Delta_p - 2V_{rr} - i\gamma/2)^{-1}. \end{aligned}$$

In particular, we are interested in having a completely local jump operator, i.e. $c_a^{(i)} = \sqrt{\gamma} |g_i\rangle\langle r_i|$ with a tunable decay rate γ . This is possible by having a large detuning to the state $|p_i\rangle$, i.e. $\Delta_p \gg V_{rr}$, resulting in all the λ_i being identical. The complex coefficient in $c_{\text{eff}}^{(m)}$ can be interpreted as an effective decay rate that is given by

$$\gamma = |\langle g_m | c_{\text{eff}}^{(m)} | r_m \rangle|^2 = \frac{\Omega_{\text{AUX}}^2}{\Delta_p^2 + \gamma_p^2/4} \gamma_p. \quad (\text{S8})$$

For the experimental parameters given in the main text, we have $V_{rr} = 2\pi \times 120$ MHz, which for $\Delta_p = 2\pi \times 500$ MHz results in $\Omega_{\text{AUX}} = 2\pi \times 80$ MHz, which is well achievable for a low-lying Rydberg state like $|29S_{1/2}\rangle$.

Furthermore, we wish to note that we have assumed a two-photon excitation scheme connecting the ground state to the Rydberg state, in order to have a dipole-allowed transition between the Rydberg and the intermediate state. However, it is also possible to work with P Rydberg states following a single-photon excitation, by replacing Ω_{AUX} by a two-photon process combining the last two stages of three-photon Rydberg excitation schemes [3, 4].

S.2. VARIATIONAL TREATMENT OF LONG-RANGE CORRELATIONS

S.2.1. Derivation of the variational cost function

Here, we extend the variational principle for dissipative many-body systems to the regime of long-range interactions and correlations. Regarding the variational ansatz, we only include two-body long-range correlations and ignore higher-order correlations. This is justified according to the Bogoliubov-Born-Green-Kirkwood-Yvon hierarchy for correlation operators [5], asserting that in dissipative dynamics higher-order correlations decay faster than two-body terms. The variational ansatz is given by

$$\rho_{\text{var}} = \prod_{i=1}^N \rho_i + \sum_{i < j} \mathcal{R} C_{ij}, \quad (\text{S9})$$

where $C_{ij} = \rho_{ij} - \rho_i \otimes \rho_j$ denotes long-range correlations. For spin-1/2 systems, we can express the generic form of ρ_i and C_{ij} in terms of the Pauli matrices

$$\rho_i = \frac{1}{2} \left(\mathbb{1}_i + \sum_{\mu \in \{x, y, z\}} \alpha_\mu \sigma_\mu^{(i)} \right), \quad (\text{S10a})$$

$$C_{ij} = \frac{1}{4} \sum_{\substack{\mu, \nu \in \\ \{x, y, z\}}} \zeta_{ij}(\mu, \nu) \sigma_\mu^{(i)} \sigma_\nu^{(j)}. \quad (\text{S10b})$$

where α_μ denote the variational parameters and $\zeta_{ij}(\mu, \nu)$ represent variational correlation functions. Importantly, one has to define variational functions such that they preserve long-range effects of correlations but while keeping the number of variational parameters as low as possible in order to reduce numerical complexity of minimization. To this end, the variational correlation functions can be chosen based on prior knowledge about the stationary properties of the model we wish to analyze.

Regarding the variational cost function, we base our definition according to the Hilbert-Schmidt norm that reads as

$$F_v \equiv \frac{\|\mathcal{L}\rho_{\text{var}}\|_{\text{HS}}^2}{N \|\rho_{\text{var}}\|_{\text{HS}}^2}, \quad (\text{S11})$$

which is normalised by the system size N to have an intensive quantity and also the totally purity $\|\rho_{\text{var}}\|_{\text{HS}}^2$ to makes the Hilbert-Schmidt norm unbiased towards any certain class of quantum states [6]. To find an efficiently computable variational norm, we expand the Liouvillian in terms of local and interacting terms, i.e. $\mathcal{L} = \sum_i \mathcal{L}_i + \frac{1}{2} \sum_{i \neq j} \mathcal{L}_{ij}$, where in the latter for the sake of simplicity we assume binary interactions. For the numerator of F_v , we exploit the inner-product representation of the HS norm, i.e.

$$\begin{aligned} \|\mathcal{L}\rho\|_{\text{HS}}^2 &= \langle\langle \rho_{\text{var}} | \mathcal{L}^\dagger \mathcal{L} | \rho_{\text{var}} \rangle\rangle \\ &= \langle\langle \rho_{\text{var}} | \sum_{i \neq j} \sum_{k \neq l} (\mathcal{L}_i + \frac{1}{2} \mathcal{L}_{ij})^\dagger (\mathcal{L}_k + \frac{1}{2} \mathcal{L}_{kl}) | \rho_{\text{var}} \rangle\rangle \\ &\approx N \sum_{1 \neq j \neq k \neq l} G_p^{1jkl} \langle\langle \rho_{\text{var}}^{(1jkl)} | \mathcal{L}_1^\dagger \mathcal{L}_1 + \mathcal{L}_1^\dagger \mathcal{L}_j + 2\mathcal{L}_1^\dagger \mathcal{L}_{1j} + \frac{1}{2} \mathcal{L}_{1j}^\dagger \mathcal{L}_{1j} \\ &\quad + \mathcal{L}_1^\dagger \mathcal{L}_{jk} + \frac{1}{2} \mathcal{L}_{1j}^\dagger \mathcal{L}_{jk} + \frac{1}{2} \mathcal{L}_{1j}^\dagger \mathcal{L}_{1k} + \frac{1}{4} \mathcal{L}_{1j}^\dagger \mathcal{L}_{kl} | \rho_{\text{var}}^{(1jkl)} \rangle\rangle \end{aligned} \quad (\text{S12})$$

where $G_p^{ijkl} = \langle\langle \rho_{\text{var}}^{ijkl} | \rho_{\text{var}}^{ijkl} \rangle\rangle$ is the purity of the given density matrix corresponding to $N - 4$ sites excluding sites $\{i, j, k, l\}$ and

$$g_p = \langle\langle \rho_1 | \rho_1 \rangle\rangle = (1 + \alpha_x^2 + \alpha_y^2 + \alpha_z^2)/2, \quad (\text{S13})$$

is the single-site purity. The approximation in Eq. (S12) comes from the exclusion of the marginal correlations, i.e. we assume $\rho_{\text{var}}^{(ijklm)} = \rho_{\text{var}}^{(ijkl)} \otimes \rho_{\text{var}}^{(m)}$. We have also made the assumption that the underlying system exhibits translational symmetry.

Finally, the variational cost function can be expressed as in the following form,

$$F_v = G_p^{-1} \left[\sum_{1 \neq j \neq k \neq l} G_p^{1jkl} \langle \rho_{\text{var}}^{(1jkl)} | \mathcal{L}_1^\dagger \mathcal{L}_1 + \mathcal{L}_1^\dagger \mathcal{L}_j + 2\mathcal{L}_1^\dagger \mathcal{L}_{1j} + \frac{1}{2} \mathcal{L}_{1j}^\dagger \mathcal{L}_{1j} \right. \\ \left. + \mathcal{L}_1^\dagger \mathcal{L}_{jk} + \frac{1}{2} \mathcal{L}_{1j}^\dagger \mathcal{L}_{jk} + \frac{1}{2} \mathcal{L}_{1j}^\dagger \mathcal{L}_{1k} + \frac{1}{4} \mathcal{L}_{1j}^\dagger \mathcal{L}_{kl} | \rho_{\text{var}}^{(1jkl)} \rangle \right]. \quad (\text{S14})$$

This equation is still computationally very intensive even for small lattices. Therefore, we find a more efficient function which is an upper bound to the variational cost function,

$$F_v \leq f_v = g_p^{-2} \sum_{1 \neq j} \langle \rho_{\text{var}}^{(1j)} | \mathcal{L}_1^\dagger \mathcal{L}_1 + \mathcal{L}_1^\dagger \mathcal{L}_j | \rho_{\text{var}}^{(1j)} \rangle \\ + g_p^{-3} \sum_{1 \neq j \neq k} \langle \rho_{\text{var}}^{(1jk)} | 2\mathcal{L}_1^\dagger \mathcal{L}_{1j} + \mathcal{L}_1^\dagger \mathcal{L}_{jk} | \rho_{\text{var}}^{(1jk)} \rangle \\ + g_p^{-4} \sum_{1 \neq j \neq k \neq l} \langle \rho_{\text{var}}^{(1jkl)} | \frac{1}{2} \mathcal{L}_{1j}^\dagger \mathcal{L}_{1j} + \frac{1}{2} \mathcal{L}_{1j}^\dagger \mathcal{L}_{jk} + \frac{1}{2} \mathcal{L}_{1j}^\dagger \mathcal{L}_{1k} + \frac{1}{4} \mathcal{L}_{1j}^\dagger \mathcal{L}_{kl} | \rho_{\text{var}}^{(1jkl)} \rangle, \quad (\text{S15})$$

where here we made the approximation that $G_p(N) \approx G_p(N - n)g_p^n$ which is valid for $N \gg n$. Here, n denotes the dimension of the variational states ρ_{var} appearing in the variational norm.

S.2.2. Simplifying the upper bound

In the following, we will present further simplifications reducing the number of variational parameters in two different ways, by incorporating prior knowledge of the details of the long-range interacting Rydberg model. First, we introduce a pair correlation function to capture the correlations between different Rydberg excitation, which has a form that follows from prior knowledge from Rydberg-blockaded systems. Second, we employ the Heisenberg equations of motion to remove some of the variational parameters.

1. Variational correlation functions

The Rydberg blockade manifests itself in the two-body correlation among Rydberg states qualified by the well-known pair correlation function g_2 which reads

$$g_2(r) = \frac{\sum_{i \neq j} g_2(i, j) \delta(r_{ij} - r)}{\sum_{i \neq j} \delta(r_{ij} - r)}, \quad (\text{S16})$$

with

$$g_2(i, j) = \frac{\langle P_r^{(i)} P_r^{(j)} \rangle}{\langle P_r^{(i)} \rangle \langle P_r^{(j)} \rangle}. \quad (\text{S17})$$

The g_2 function is strongly suppressed within the blockade volume where no simultaneous Rydberg excitation can take place, i.e. $\langle P_r^{(i)} P_r^{(j)} \rangle \sim r^6$ for small values of r . On the other hand, for long enough distances the (Rydberg density-density) correlation vanishes, i.e. $\langle P_r^{(i)} P_r^{(j)} \rangle - \langle P_r^{(i)} \rangle \langle P_r^{(j)} \rangle = 0$, and $g_2 = 1$. Due to the strong van der Waals interaction, this function exhibits a sharp blockaded-uncorrelated transition which roughly resembles a step function with some overshooting [7]. Our ansatz for the g_2 function is

$$g_2(r) \approx \frac{\tilde{r}^6}{\tilde{r}^6 + \alpha_{zz}^{(1)} + \alpha_{zz}^{(2)} \tilde{r} + \alpha_{zz}^{(3)} \tilde{r}^2}, \quad (\text{S18})$$

correlation function	variational parameters	variational ansatz
$\zeta_{ij}(x, x)$	$\alpha_{xx}^{(1)}, \alpha_{xx}^{(1)}$	$\alpha_{xx}^{(2)} \exp[-\alpha_{xx}^{(2)} r_{ij}]$
$\zeta_{ij}(y, y)$	$\alpha_{yy}^{(1)}, \alpha_{yy}^{(1)}$	$\alpha_{yy}^{(2)} \exp[-\alpha_{yy}^{(2)} r_{ij}]$
$\zeta_{ij}(z, z)$	$\alpha_z, \alpha_{zz}^{(1)}, \alpha_{zz}^{(2)}, \alpha_{zz}^{(3)}, \alpha_{zz}^{(4)}$	$[g_2(r) - 1](\alpha_z + 1)^2$
$\zeta_{ij}(x, y)$	$\alpha_{xy}^{(1)}, \alpha_{xy}^{(2)}$	$\alpha_{xy}^{(1)} \exp[-\alpha_{xy}^{(2)} r_{ij}]$
$\zeta_{ij}(x, z)$	$\alpha_{xz}^{(1)}, \alpha_{xz}^{(2)}$	$\alpha_{xz}^{(1)} \exp[-\alpha_{xz}^{(2)} r_{ij}]$
$\zeta_{ij}(y, z)$	$\alpha_z, \alpha_{zz}^{(2)}, \alpha_{zz}^{(2)}, \alpha_{zz}^{(3)}, \alpha_{zz}^{(4)}$	$(\gamma_a + \gamma_p)[g_2(r) - 1](\alpha_z + 1)^2/\Omega$

TABLE II. Variational ansatz for two-body correlation functions in two-dimensional driven-dissipative Rydberg gases.

where $\tilde{r} \equiv \alpha_{zz}^{(4)} r$ in which α 's are the corresponding variational parameters. This function satisfies both limits for small and large values of r . Using this simple function, we can estimate the long-range correlations in driven-dissipative Rydberg gases while keeping the number of variational parameters as low as possible. In particular, the parameter $\alpha_{zz}^{(4)}$ controls the value of the blockade radius, while the remaining parameters account for the details of the shape.

Now, one can easily express the zz correlation function, i.e. $\zeta_{ij}(z, z) \equiv \langle \sigma_z^{(i)} \sigma_z^{(j)} \rangle - \langle \sigma_z^{(i)} \rangle \langle \sigma_z^{(j)} \rangle$, by expressing the definition of $g_2(r_{ij})$ in terms of σ_z . Crucially, we exploit translational invariance of the system, i.e., $\alpha_z = \langle \sigma_z^{(i)} \rangle \simeq \langle \sigma_z^{(j)} \rangle$. As a result, our variational ansatz for zz correlation function is given by

$$\zeta_{ij}(z, z) = [g_2(r_{ij}) - 1](\alpha_z + 1)^2. \quad (\text{S19})$$

Using the Heisenberg equations of motion we can further decrease the number of variational parameters. In the case of the dissipative Rydberg model, one can find closed relations between some variational parameters by solving the corresponding Heisenberg equations for the steady state solution,

$$\begin{aligned} \frac{d}{dt} \langle \sigma_z^{(i)} \rangle &= 0 \rightarrow \alpha_y = \frac{\gamma_a}{\Omega} (\alpha_z + 1), \\ \frac{d}{dt} \langle \sigma_z^{(i)} \sigma_z^{(j)} \rangle &= 0 \rightarrow \zeta_{ij}(y, z) = \frac{\gamma_a + \gamma_p}{\Omega} \zeta_{ij}(z, z), \\ \frac{d}{dt} \langle \sigma_x^{(i)} \rangle &= 0 \rightarrow \alpha_x = \frac{\gamma_a(\alpha_z + 1)}{\Omega(\gamma_a + 4\gamma_p)} \left[2\Delta - C_6(\alpha_z + 1) \sum_{j \neq i} \frac{g_2(r_{ij})}{r_{ij}^6} \right], \end{aligned} \quad (\text{S20})$$

For the remaining correlation functions, we use a simple exponential decay, which is in good agreement with numerical simulations of small systems. In Table II all the aforementioned ansätze are presented. Therefore, in total we have formulated the variational many-body state in terms of 13 parameters.

It is worth mentioning that our variational ansatz is mostly expanded around the diagonal elements of the density matrix. This is because all the variational correlation functions are exponentially decaying with the distance except the zz and yz correlation functions that only contribute to diagonal and semi-diagonal elements respectively (see Table II). This is consistent with the reported Monte-Carlo simulation of the dynamics showing that the dissipative processes destroy quantum correlations while enhancing classical correlations [8]. As a result, the long-time limit of the total density matrix is nearly diagonal.

2. Minimization constraints

Having fixed the variational manifold, we have to choose a proper minimization method to be able to find the optimal solution for the associated steady state. In this specific model, since the variational landscape is relatively benign, we make use of a fast-converging local non-linear optimization method based on the gradient-descent scheme. In particular, we use SLSQP Optimization subroutine of SciPy library in Python [9]. The implemented SLSQP method supports constrained optimization which is necessary for the variational method as discussed below.

Specifically, the minimization of the variational norm is constrained by two inequalities. The first inequality ensures the positivity of the quantum state. Additionally, we impose a second inequality constraint derived from the ansatz for the pair correlation function. Explicitly, these inequalities are given by

1. Positivity of the density matrix ρ : As the variational norm consists of bipartite reduced density matrices, we only have positivity constraints on all these matrices

$$\langle\langle \rho_{ij} | \Psi \rangle\rangle \geq 0 \quad \text{for any } |\Psi\rangle,$$

that $\rho_{ij} = \text{Tr}_{\mathcal{H}}[\rho]$. From numerical point of view, this constraint is equivalent to the positivity of the smallest eigenvalue of ρ_{ij} ,

$$E_1[\rho_{ij}] \geq 0 \quad \text{for all } \rho_{ij}.$$

2. Normalization condition: In equilibrium, normalization condition of the pair correlation function $g_2(\mathbf{r})$ leads to $\int d\mathbf{r}[1 - g_2(\mathbf{r})] = \langle P_r \rangle^{-1}$ [10]. In the non-equilibrium case, this equality condition turns into the following inequality constraint

$$\sum_{i \neq j} r_{ij} [1 - g_2(\mathbf{r})] \leq \frac{1}{\langle P_r \rangle}.$$

S.3. EFFECTIVE SHORT-RANGE DESCRIPTION OF FROZEN RYDBERG GASES

The Rydberg Hamiltonian resembles the transverse-field Ising Hamiltonian with long-range interactions, i.e.

$$H_{\text{Ising}} = \frac{\Omega}{2} \sum_i \sigma_x^{(i)} + V \sum_{i < j} \frac{\sigma_z^{(i)} \sigma_z^{(j)}}{|\mathbf{r}_i - \mathbf{r}_j|^6}. \quad (\text{S21})$$

However, there are two differences between these two Hamiltonians. First, the Ising interaction $\sigma_z^{(i)} \sigma_z^{(j)}$ does not exclude ground state interactions as the Rydberg-Rydberg interaction does. Second, the Rydberg Hamiltonian contains additional terms proportional to $\sigma_z^{(i)}$ which corresponds to a longitudinal magnetic field in the spin language. However, by expanding Rydberg interactions in terms of σ_z , one can obtain Ising interactions and cancel out the longitudinal field by an effective detuning. Nevertheless, reducing Rydberg interactions to Ising ones may destroy the particular properties of Rydberg gases such as the blockade effect. Hence, we effectively mimic the blockade by discarding sites up to a truncation radius r_d and keeping the subsequent long-range tail in an Ising form. This approach can be seen as a long-range extension of so-called “perfect blockade” models [11, 12]. Then, we obtain

$$\begin{aligned} H_{\text{Ryd}} = & -\frac{\Delta}{2} \sum_i \sigma_z^{(i)} + \frac{\Omega}{2} \sum_i \sigma_x^{(i)} + \frac{C_6}{a^6} \sum_{r_{ij} \leq r_d} \frac{P_r^{(i)} P_r^{(j)}}{r_{ij}^6} \\ & + \frac{C_6}{4a^6} \sum_{r_{ij} > r_d} \frac{\sigma_z^{(i)} + \sigma_z^{(j)}}{r_{ij}^6} + \frac{C_6}{4a^6} \sum_{r_{ij} > r_d} \frac{\sigma_z^{(i)} \sigma_z^{(j)}}{r_{ij}^6} + \frac{C_6}{4a^6} \sum_{r_{ij} > r_d} \frac{\mathbf{1}^{(i)} \mathbf{1}^{(j)}}{r_{ij}^6}, \end{aligned} \quad (\text{S22})$$

where $r_{ij} = |\mathbf{r}_i - \mathbf{r}_j|$. Since the last term only shifts the total energy of the system, we can ignore it. Hence, we have

$$\begin{aligned} H_{\text{Ryd}} = & \left(-\frac{\Delta}{2} + V_z \right) \sum_i \sigma_z^{(i)} + \frac{\Omega}{2} \sum_i \sigma_x^{(i)} \\ & + \frac{C_6}{a^6} \sum_{r_{ij} \leq r_d} \frac{P_r^{(i)} P_r^{(j)}}{r_{ij}^6} + \frac{C_6}{4a^6} \sum_{r_{ij} > r_d} \frac{\sigma_z^{(i)} \sigma_z^{(j)}}{r_{ij}^6}, \end{aligned} \quad (\text{S23})$$

where

$$V_z = \frac{C_6}{4a^6} \sum_{r_{ij} > r_d} \frac{1}{r_{ij}^6}, \quad (\text{S24})$$

represents the interaction-induced shift in the longitudinal magnetic field.

r_d	$V_z a^6 / C_6$	$\Delta / 2\pi [\text{MHz}]$
0	$\zeta(3)\beta(3)$	2055.0144
1	$\zeta(3)\beta(3) - (1)$	290.6422
$\sqrt{2}$	$\zeta(3)\beta(3) - (1 + \frac{1}{8})$	70.0957
2	$\zeta(3)\beta(3) - (1 + \frac{1}{8} + \frac{1}{64})$	42.5274
$\sqrt{5}$	$\zeta(3)\beta(3) - (1 + \frac{1}{8} + \frac{1}{64} + \frac{2}{125})$	14.2974
$\sqrt{8}$	$\zeta(3)\beta(3) - (1 + \frac{1}{8} + \frac{1}{64} + \frac{2}{125} + \frac{1}{512})$	10.8514
3	$\zeta(3)\beta(3) - (1 + \frac{1}{8} + \frac{1}{64} + \frac{2}{125} + \frac{1}{512} + \frac{1}{729})$	8.4311

TABLE III. Transverse points of the laser detuning in the Rydberg Hamiltonian for $C_6 = h \times 20\text{MHz}\mu\text{m}^6$ and $a = 532\text{nm}$.

As mentioned before, we can cancel out the longitudinal field by an appropriate choice of the detuning, i.e., $\Delta(r_d) = 2V_z(r_d)$. Crucially, at the extreme case of $r_d = 0$, the resulting value of detuning $\Delta(r_d = 0)$ is very large such that it compensates for the energy shift by the strong vdW interaction, leading to the anti-blockade regime. However, we are interested in the regime of finite r_d where the Rydberg blockade plays an important role. In the following, we refer to these values of detuning as transverse points. To quantify these points, let's first evaluate the V_z which is related to r_d as following

$$V_z(r_d) = \frac{C_6}{4a^6} \left[\sum'_{r_{ij}=-\infty}^{+\infty} \frac{1}{r_{ij}^6} - \sum_{r_{ij} \leq r_d} \frac{1}{r_{ij}^6} \right], \quad (\text{S25})$$

where the primed sum indicates that the zero point is excluded. Using the notion of Dirichlet series, the first term of the above equation describing distances on a square lattice, is equivalent to

$$\begin{aligned} \sum'_{-\infty}^{+\infty} \frac{1}{r_{ij}^6} &= \sum'_{-\infty}^{+\infty} \frac{1}{(i^2 + j^2)^3} \\ &= 4\zeta(3)\beta(3), \end{aligned} \quad (\text{S26})$$

where $\beta(x)$ is the Dirichlet β -function and $\zeta(x)$ is the Riemann ζ -function [13]. We recall that $\beta(3) = \pi^3/32$ and $\zeta(3) \approx 1.202057$ is the sum of the reciprocals of the positive cubes which is known as the Apéry's constant. Therefore, we can express Eq. (S25) as follows

$$V_z = \frac{C_6}{a^6} \left[\zeta(3)\beta(3) - \sum_{r_{ij} \leq r_d} \frac{f(i, j)}{r_{ij}^6} \right], \quad (\text{S27})$$

where

$$f(i, j) = \begin{cases} 2 & \text{if } i \neq 0 \text{ and } i \neq j, \\ 1 & \text{otherwise.} \end{cases}$$

In Table III, we present the transverse points of the laser detuning for $0 < r_d < 3$ and the nearest-neighbor interaction strength of $C_6/a^6 \approx h \times 882\text{MHz}$.

To proceed further, it is possible to have an effective low-energy description of the aforementioned model with the associated truncation radius r_d . A short-range Ising model can be used as an effective model with the Hamiltonian,

$$H_{\text{eff}} = h_z(r_d) \sum_i \sigma_z^{(i)} + \frac{\Omega}{2} \sum_i \sigma_x^{(i)} + J_{\text{eff}}(r_d) \sum_{\langle ij \rangle} \sigma_z^{(i)} \sigma_z^{(j)}, \quad (\text{S28})$$

with $h_z(r_d) = -\Delta/2 + V_z$ and $J_{\text{eff}}(r_d) = V_z$. This effective model is a good candidate for describing the original model

at the transverse points, i.e. $h_z(r_d) = 0$.

-
- [1] C. Nill, K. Brandner, B. Olmos, F. Carollo, and I. Lesanovsky, Many-body radiative decay in strongly interacting Rydberg ensembles (2022), [arXiv:2206.02843 \[quant-ph\]](#).
 - [2] F. Reiter and A. S. Sørensen, Effective operator formalism for open quantum systems, [Phys. Rev. A **85**, 032111 \(2012\)](#).
 - [3] J. H. Gurian, P. Cheinet, P. Huillery, A. Fioretti, J. Zhao, P. L. Gould, D. Comparat, and P. Pillet, Observation of a Resonant Four-Body Interaction in Cold Cesium Rydberg Atoms, [Phys. Rev. Lett. **108**, 023005 \(2012\)](#).
 - [4] V. M. Entin, E. A. Yakshina, D. B. Tretyakov, I. I. Beterov, and I. I. Ryabtsev, Spectroscopy of the three-photon laser excitation of cold Rubidium Rydberg atoms in a magneto-optical trap, [J. Exp. Theor. Phys. **116**, 721 \(2013\)](#).
 - [5] P. Navez and R. Schützhold, Emergence of coherence in the Mott-insulator–superfluid quench of the Bose-Hubbard model, [Phys. Rev. A **82**, 063603 \(2010\)](#).
 - [6] J. Kazemi and H. Weimer, Genuine Bistability in Open Quantum Many-Body Systems, [arXiv:2111.05352 \(2021\)](#).
 - [7] R. Löw, H. Weimer, J. Nipper, J. B. Balewski, B. Butscher, H. P. Büchler, and T. Pfau, An Experimental and Theoretical Guide to Strongly Interacting Rydberg Gases, [J. Phys. B: At. Mol. Opt. Phys. \(2012\)](#).
 - [8] D. Petrosyan, M. Hönig, and M. Fleischhauer, Spatial correlations of Rydberg excitations in optically driven atomic ensembles, [Phys. Rev. A **87**, 053414 \(2013\)](#).
 - [9] P. Virtanen *et al.*, SciPy 1.0: Fundamental Algorithms for Scientific Computing in Python, [Nature Methods **17**, 261 \(2020\)](#).
 - [10] H. Weimer, R. Löw, T. Pfau, and H. P. Büchler, Quantum Critical Behavior in Strongly Interacting Rydberg Gases, [Phys. Rev. Lett. **101**, 250601 \(2008\)](#).
 - [11] B. Sun and F. Robicheaux, Numerical study of two-body correlation in a 1D lattice with perfect blockade, [New J. Phys. **10**, 045032 \(2008\)](#).
 - [12] B. Olmos, M. Müller, and I. Lesanovsky, Thermalization of a strongly interacting 1D Rydberg lattice gas, [New Journal of Physics **12**, 013024 \(2010\)](#).
 - [13] A. Actor, Evaluation of multidimensional linear zeta functions, [J. Number Theor. **35**, 62 \(1990\)](#).